Laser and Particle Beams (2008), *26*, 167–178. Printed in the USA.

doi:10.1017/S0263034608000190

Ways to discharge-based soft X-ray lasers with the wavelength $\lambda < 15$ nm

K. KOLACEK, J. SCHMIDT, V. PRUKNER, O. FROLOV, AND J. STRAUS
Institute of Plasma Physics, Academy of Sciences of the Czech Republic, Prague, Czech Republic
(RECEIVED 11 November 2007; ACCEPTED 6 March 2008)

Abstract

Two basic ways to amplification of spontaneous emission in the soft X-ray region are described. The first is based on the electron-collisional recombination pumping scheme, which uses recombination of fully stripped ions into hydrogen-like ions to create (in the case of sufficiently fast cooling) a population inversion on energy levels belonging to the Balmer-alpha transition. We test this scheme on nitrogen, for which the lasing wavelength is 13.4 nm. The second way to amplification of spontaneous emission is based on the electron-collisional excitation pumping scheme: this uses for creation of population inversion a fast excitation of Ne- or Ni-like ions. However, for wavelength below 15 nm it is necessary to use Ni-like ions of some metal vapors. Feeding metal vapors into a capillary is difficult, and if being fed they deposit on the capillary wall and significantly reduce the capillary lifetime. That is why we prepare metal vapor plasma in a capillary with liquid wall – by wire explosion in water. For slowdown of the plasma-channel expansion a local-water-compression by linearly focused shock wave is being developed.

Keywords: Capillary discharges; Exploding wires in water; Focused shock waves in water; Soft X-ray lasers

INTRODUCTION

At present there is a strong interest in high energy density physics and X-ray generation with reliable pulsed power devices (Milani *et al.*, 2007; Orlov *et al.*, 2007; Wong *et al.*, 2007; Zou *et al.*, 2006) and in a shortening of the wavelength of discharge pumped soft X-ray lasers. There are four possible ways (Kolacek, 2002), how to achieve population inversion with pulse power devices—namely with the help of recombination, of excitation by discharge itself, of combined excitation by discharge, and pico-/femto-second laser pulse, and finally with the help of charge exchange; three of them seem to be feasible even in the case of shorter wavelength.

The first way to population inversion is usually used in evacuated small diameter capillaries, where the discharge is initiated by a surface breakdown along the capillary wall. Such a breakdown does not ensure well-defined initial conditions (the number of from wall-evaporated particles is uncontrolled), but plasma remains in good thermal contact with capillary walls and amplification of spontaneous emission (usually during a cooling phase of the discharge—following electron-collisional recombination pumping scheme into hydrogen- or lithium-like ions) has been reported (Boss *et al.*, 1998; Eberl *et al.*, 1997; Shin *et al.*, 1994; Steden & Kunze, 1990; Wagner *et al.*, 1996*a*, 1996*b*). Later it was noticed (Kirsch *et al.*, 2001) that lasing conditions according to the recombination pumping scheme were approached in ultrafast gas-filled micro-capillary discharge device with stored energy as small as 0.5 J: the gas is ionized along the capillary axis by an electron beam (due to hollow cathode effect) and a 1-ns discharge heats the plasma to a temperature >80 eV. Recently, following general considerations of Z-scaling (Z being atomic number) of capillary gas-filling (Lee *et al.*, 2002), an amplification on H-like N (Balmer-alpha-line, wavelength 13,4 nm—see Fig. 1) in N-filled capillary of larger diameter (~3 mm) has been predicted (Vrba *et al.*, 2005*a*, 2005*b*; Vrba & Vrbova, 2006). Experimental tests of these calculations are in progress (Jancarek *et al.*, 2006).

The second way to population inversion in capillary discharge devices was found in gas filled capillaries with massive pre-ionization and a fast current rise-time. In this case, the amount of material ablated from the capillary walls and, hence, the number of particles to be heated, is limited by a rapid detachment of plasma from the walls (by Z-pinch effect). Strong amplification (Rocca *et al.*, 1993;

Address correspondence and reprint requests to: K. Kolacek, Institute of Plasma Physics, Academy of Sciences of the Czech Republic, v.v.i., Za Slovankou 3, 182 00 Prague 8, Czech Republic. E-mail: kolacek@ipp.cas.cz

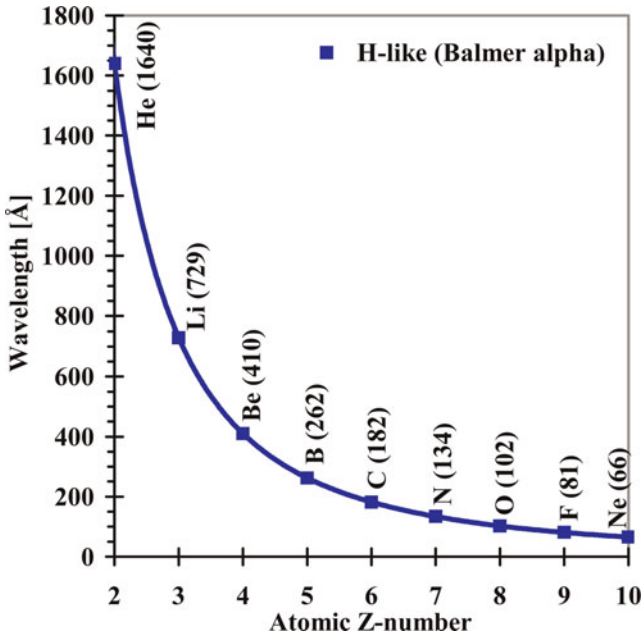

Fig. 1. (Color online) Wavelengths of hydrogen-like ions (Balmer-alpha transition) for elements with different atomic numbers.

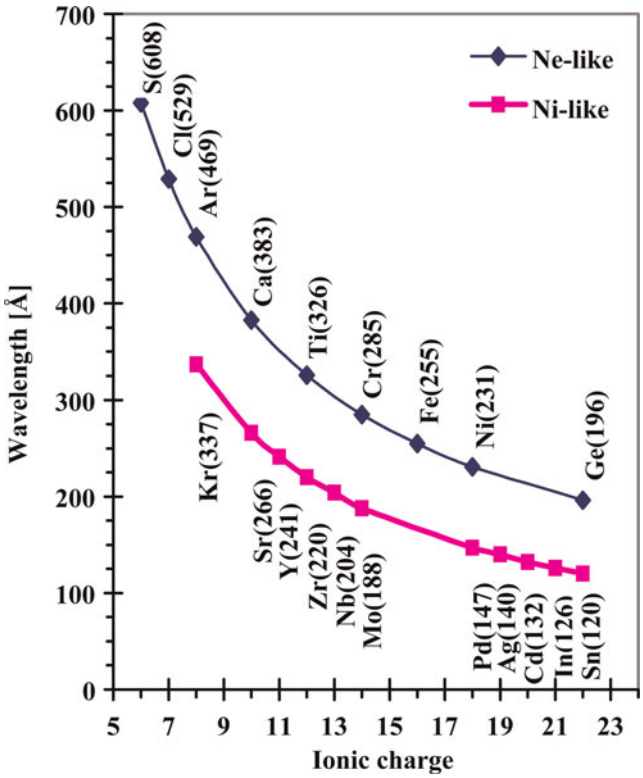

Fig. 2. (Color online) Lasing wavelengths for Ne- and Ni-like ions as a function of ionic charge.

Hildebrand *et al.*, 1996) (due to electron-collisional excitation pumping scheme, which prefers neon- or nickel-like ions), lasing (Rocca *et al.*, 1994; Ben-Kish *et al.*, 2001; Tomassetti *et al.*, 2002; Hayashi *et al.*, 2003) and achievement of saturation limit (Rocca *et al.*, 1996*a*, 1996*b*; Tomassetti *et al.*, 2004; Ritucci *et al.*, 2004) with neon-like argon (46.9 nm) have been announced in a short time interval. Later lasing on neon-like sulphur (60.8 nm) (Tomasel *et al.*, 1997; Rocca *et al.*, 1997), and neon-like chlorine (52.9 nm) (Frati *et al.*, 2000) were demonstrated. However, shortening of lasing wavelength has not yet been successful: it requires to use Ne-, or better Ni-like ions of metal vapors (see Fig. 2). While injection of metal vapor plasma into the capillary is difficult (Rahman *et al.*, 2003; Frati *et al.*, 2001), the delivery of Ag atoms into the capillary by ablation of its Ag_2S wall (Wang *et al.*, 2005), or the delivery of Ti atoms into the capillary by ablation of segmented Ti ring structure within the capillary (Wyndham *et al.*, 2006), or by Ti-wire explosion (Shuker *et al.*, 2006), might be feasible. However, in all these cases, the metal vapor deposits on the capillary wall and significantly reduces its lifetime. Therefore, we suggest (similarly as Sasaki *et al.*, 2006) creating a metal vapor plasma channel with liquid wall by wire explosion in a liquid (water). A threat of fast channel expansion will be mitigated by a local liquid compression (to the GPa pressure range) by linearly focused cylindrical shock wave.

The third way to population inversion is hybrid pumping scheme, which combines generation and compression of plasma by discharge, and build-up of population inversion by a pico- or femto-second laser pulse. The wave-guiding of high intensity laser pulses in straight and curved plasma channels has been known for a few years (Ehrlich *et al.*, 1996; Hosokai *et al.*, 1999; Kaganovich *et al.*, 1999; Bobrova *et al.*, 2000; Goltsov *et al.*, 2000), as well as the idea of amplification of a soft X-ray laser beam in active medium (Chilla & Rocca, 1996), but the feasibility of this scheme was demonstrated quite recently (Janulewicz *et al.*, 2000, 2001; Nickles *et al.*, 2001). This approach is studied up to now both theoretically (Janulewicz *et al.*, 2003) and experimentally (Luther *et al.*, 2005; Janulewicz *et al.*, 2005). We consider it promising; unfortunately, up to the present, laser delivered the prevailing part of the energy. That disqualifies smaller laboratories. We think it is worth testing this scheme with a laser of energy/power just slightly higher than that necessary for excitation of the upper laser level.

The fourth way to population inversion in capillary devices is the charge exchange pumping scheme (Kunze *et al.*, 1994). Because such a pumping is quite unusual—it was independently tested using two colliding plasma streams originating in two laser foci (0.75 mm apart) (Ruhl *et al.*, 1997) and modeled (Koshelev & Kunze, 1997). Despite initial objections (Boboc *et al.*, 2000—intensity enhancement in the former experiments was interpreted in terms of guiding effect rather than by amplified spontaneous emission), the method of externally induced instabilities (the number of which equals to number of circular trenches in inner capillary wall (Ellwi *et al.*, 2001*a*, 2001*b*; Kunze *et al.*, 2006)) fully confirms amplification of spontaneous

https://doi.org/10.1017/S0263034608000190 Published online by Cambridge University Press

emission. Recently, the same effect was achieved by modulated return conductor (Kunze *et al.*, 2005). However, we expect the general applicability of this scheme to scaling down the lasing wavelength is very small.

From the above given survey, it is seen that with the excitation pumping scheme the best results to date have been obtained. These experiments have the highest energy in pulse, peak power, and average power in repetitive regime, they demonstrated lasing at more wavelengths, their X-ray laser beam was examined (near and far field pattern, coherence) and used for the first applications. However, because the energy difference between lasing levels (upper and lower) scales with ionic charge in case of the recombination pumping more rapidly than in case of the excitation pumping (compare Fig. 1 and Fig. 2), both these pumping schemes remain in the focus of our interest.

X-RAY AMPLIFICATION CONDITIONS

Power

If N_u and N_l are upper and lower laser state population densities and σ_{stim} and σ_{abs} are cross-sections for stimulated emission and resonance absorption, then the small signal gain coefficient is

$$g = N_u\sigma_{stim} - N_l\sigma_{abs} \sim N_u\sigma_{stim}, \quad (1)$$

where the cross section for stimulated emission (Elton, 1990) is given by

$$\sigma_{stim} = \frac{c^2}{8\pi\nu^2}\frac{A_{ul}}{\Delta\nu}, \quad (2)$$

c being the speed of light, ν the line frequency, and $\Delta\nu$ the line width. Taking into account that Einstein coefficient for spontaneous emission A_{ul} scales along an isoelectronic sequence as λ^{-2} then (Rocca, 1999)

$$g \approx \frac{1}{8\pi\Delta\nu}N_u. \quad (3)$$

For naturally broadened line $\Delta\nu \sim A_{ul} \sim \lambda^{-2}$ and hence,

$$g_{natural} \approx N_u\lambda^2. \quad (4)$$

Maintenance of the upper laser level population density N_u requires pump power density P

$$P_{natural} = N_uA_{ul}hc/\lambda \sim N_u\lambda^{-3} \sim g_{natural}\lambda^{-5}. \quad (5)$$

For Doppler broadened line

$$\frac{\Delta\nu}{\nu} = \frac{\sqrt{kT_i/m_i}}{c}, \quad (6)$$

k being Boltzmann constant, T_i ion temperature, and m_i ion mass. Combining Eqs. (3) and (6), the gain is in this case

$$g_{Doppler} \approx \frac{1}{\sqrt{kT_i/m_i}}\frac{c}{\nu}N_u \approx \frac{\lambda}{\sqrt{kT_i/m_i}}N_u \quad (7)$$

and the "maintaining" pump power density is (using Eq. (7))

$$P_{Doppler} = N_uA_{ul}hc/\lambda \sim N_u\lambda^{-3} \sim g_{Doppler}\sqrt{kT_i/m_i}\lambda^{-4}. \quad (8)$$

Therefore, considering for illustration naturally broadened line and supposing that mirrorless operation increases power 100 times, then lasing at 50 nm requires 10^7 times higher power density than at visible 500 nm, and each next reduction of wavelength for one order of magnitude adds to power density requirement next five orders of magnitude.

Refraction Losses

Another effect limiting the gain is refraction, which bends the X-rays out of the amplifying volume, decreases the effective gain, and might limit the maximum amplification length. It also increases beam divergence and in some cases, it can cause side lobes or annular beam profiles.

In the one-dimensional (1D) case, London (1988) analyzed refraction losses in a parabolic density profile. The characteristic refraction length L_r (distance in the direction of propagation z traversed by the X-rays before being bend out) is

$$L_r = L_x\sqrt{n_{ec}/n_{e0}}, \quad (9)$$

where L_x is a transverse plasma dimension, n_{ec} is the critical density $\{n_{ec} = \pi m_e c^2/(e^2\lambda^2)\}$, and n_{e0} is the maximum electron density. Then effective gain coefficient

$$g_{eff} = g - (1/L_r). \quad (10)$$

The new "refraction gain-length" parameter defined as

$$G_r = gL_r(= g_{eff}L_r + 1) \quad (11)$$

then determines, whether exponential growth of laser power with length is maintained until saturation intensity ($G_r > 1$—in this case $g_{eff}\,L_r > 0$) or not ($G_r < 1$). Chilla and Rocca (1996) extended refraction analysis to two dimensions with cylindrical symmetry finding that the reduction of the effective gain coefficient is doubled

$$g_{eff} = g - (2/L_r). \quad (12)$$

The refraction losses can be reduced in laser pumped experiments by a special geometry of a target or by pre-pulse, in discharge pumped experiments by longitudinal magnetic field

https://doi.org/10.1017/S0263034608000190 Published online by Cambridge University Press

(Tomasel *et al.*, 1996) or by plasma waveguides (Korobkin *et al.*, 1996).

EXPERIMENTS AIMING AT RECOMBINATION PUMPING SCHEME

Apparatus

A new apparatus capillary experiment-upgrade (CAPEX-U) has been recently put in operation. It consists of oil-filled Marx generator (12.5 nF/600 kV/2.25 kJ), spacer (oil-filled), co-axial pulse forming line (Ø550 × Ø426 × 730 mm/12.7 nF/1.7 Ω), laser-triggered spark gap (Nd:YAG laser Quantel Brilliant b, 850 mJ/6 ns, split into four channels), and capillary (alumina in a polyurethane mantel, Ø40 × Ø3 × 232 mm) — see in more detail (Schmidt *et al.*, 2006) and Figure 3.

Preliminary Results

The first type of experiments was performed with a small diameter (Ø1 mm) capillary, where efficient cooling takes place. The capillary was filled with nitrogen in static regime (capillary and filling volume were separated from the detection part by a fast shutter), then the shutter was opened and a shot followed within ~1 ms. Unfortunately, even at medium current amplitude (~40 kA) the pressure in the capillary was so high that the fully ceramic capillary (wall thickness 19.5 mm) longitudinally cracked and exploded.

The second type of experiments was performed according to Vrba's and Vrbova's (2006) predictions (inner capillary-diameter ~3 mm): the apparatus was aligned, tested with Ar-filling that Ne-like Ar laser works, carefully evacuated, and at each discharge-current-amplitude from ~20 to ~80 kA the filling nitrogen pressure was changed to find the optimum pinching (indicated by a short (~ 5–10 ns) intense X-ray radiation peak detected by vacuum photodiode with a gold photocathode—see Fig. 4). Despite the fact that such a regime was in many cases found, no sharp spike (as narrow as the apparatus function of our measuring apparatus—1–2 ns) of X-ray radiation has been detected.

The spectroscopic measurements were performed with flat field spectrograph equipped with double MCP detector backed by scientific CCD camera. Their analysis (see Fig. 5) based on best-fit of the simulated and the measured spectra (Straus *et al.*, 2004, 2007) yields the plasma temperature ~110 eV, at which abundance of He-like N (N^{5+}) is present. According to our estimates approximately equal number of He-like (N^{5+}) and H-like (N^{6+}) N-ions appears at the temperature ~160 eV, while equal number of H-like (N^{6+}) and fully stripped (N^{7+}) N-ions can be found at the temperature ~200 eV. Therefore, we are still below suitable conditions for lasing, but we can still about twice increase the discharge current.

EXPERIMENTS AIMING AT EXCITATION PUMPING SCHEME

Apparatus

For these experiments, the capillary is removed from the CAPEX-U and substituted by the shock wave (SHOW) device for wire explosion in water locally compressed by a focused cylindrical shock wave (see Fig. 6). This SHOW device consists of a separate capacitor bank 18 μF/50 kV (accumulated energy 22.5 kJ), pressurized triggerable spark gap, and water-filled experimental chamber that has

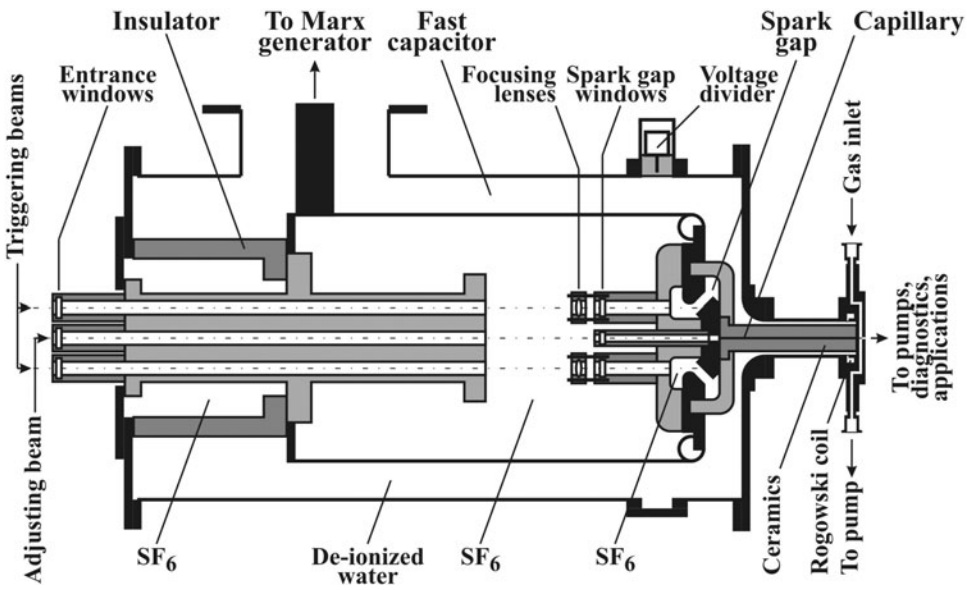

Fig. 3. CAPEX-U with a capillary.

https://doi.org/10.1017/S0263034608000190 Published online by Cambridge University Press

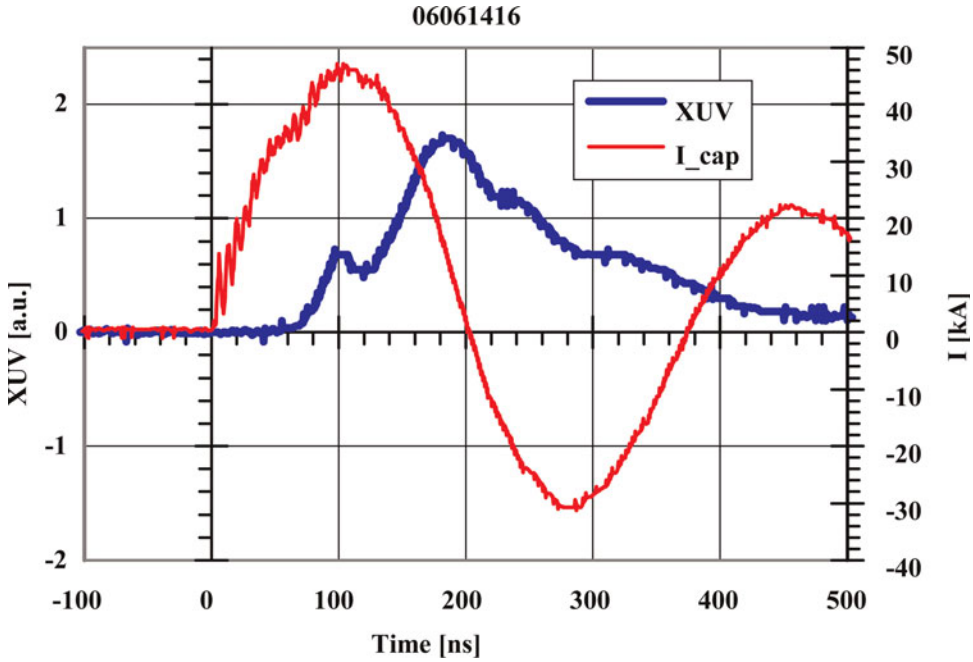

Fig. 4. (Color online) Time curves of the discharge current and the XUV radiation from the capillary filled with nitrogen.

insulating (polymethylmetacrylate (PMMA) – plexiglas) flanges and cylindrical stainless steel shell Ø400 × 200 mm serving as a ground electrode. Its inner surface is covered by a porous ceramics (almandine) that (when voltage is applied) creates strong electric field at the output of the pores, and limits the current (reducing contact of metallic wall with conducting water). The second electrode is a co-axial mesh or a foil (if water between electrodes has a higher conductivity than the rest of experimental chamber) transparent for acoustical wave. When voltage is applied the corona-like multi-streamer discharge generates a strong cylindrical acoustic wave that propagates toward the second electrode and through it further to the chamber axis. Near the axis it changes into a shock wave with strongly increasing pressure amplitude.

Pressure Measurement in/near the SHOW Focus

The Schlieren method was used for measurement of shock wave structure away from the SHOW focus. Unfortunately, the shock wave induced inhomogeneity at the focus was so large that the deflected beams went out of the schlieren lens aperture.

Off-axis shadowgraphy (newly developed technique) overcomes the above mentioned problem. The expanded laser beam (second harmonic of Nd:YAG) was directed along the axis of the separately standing SHOW device. The imaging lens ($f = 310$ mm/Ø80 mm) shielded by horizontal slit (57 × 20 mm) was placed in off-axis position to use for imaging the rays with higher deflections than in the Schlieren method (undeflected rays do not fall into lens-aperture at all (see Fig. 7)). Such measurements (an example is shown in Fig. 7, right) were repeated for a few off-axis positions and for a few delays to find the deflection, at which the signal disappears. From this deflection the maximum pressure in the inhomogeneity was inferred to be ~30 MPa at 20 kV charging voltage. A slight disagreement with pressure estimate made according to Kolacek *et al.* (2005) (70 MPa) is attributed to boundary layer effects that were neglected during the evaluation. The probing-laser-delay after the discharge and the radii of curvature of individual arcs on the shadowgrams gave the position of individual shock-wave-phases in the given time (see Fig. 8). From the graph the radius of shock wave focus 2.8 mm, and focusing time 122–125 μs after the multi-streamer discharge were determined.

A piezoelectric pressure sensor was cut from silver-ink-metallized piezo-film sheet (MSI sensors), contacted by a conducting glue, fixed on a plastic (PMMA) rod of the diameter 10 mm and placed on the SHOW axis. This piezoelectric sensor was connected to high-impedance input of a near-by battery-powered oscilloscope. The signals were smaller than expected (see Fig. 9, left), probably because the sensor thickness (110 μm) was small in comparison with characteristic dimension of the shock wave (~ 3.5 mm). The truncated signal is because of sparking.

A fiber-optic pressure sensor is based on the idea of a change in fiber transmission due to pressure-induced change of ratio of cladding/core index of refraction. The fiber (core: quartz, Ø210 μm, index of refraction $n_{core} =$ 1,457, cladding: plastic, Ø250 μm, index of refraction $n_{clad} = 1{,}41 - 1{,}44$) was selected to have as close n_{core} to n_{clad} as possible. The fiber was elastically mounted on the axis of SHOW (to exclude fiber stretching due to pressure-induced axial movement of flanges). The fiber

https://doi.org/10.1017/S0263034608000190 Published online by Cambridge University Press

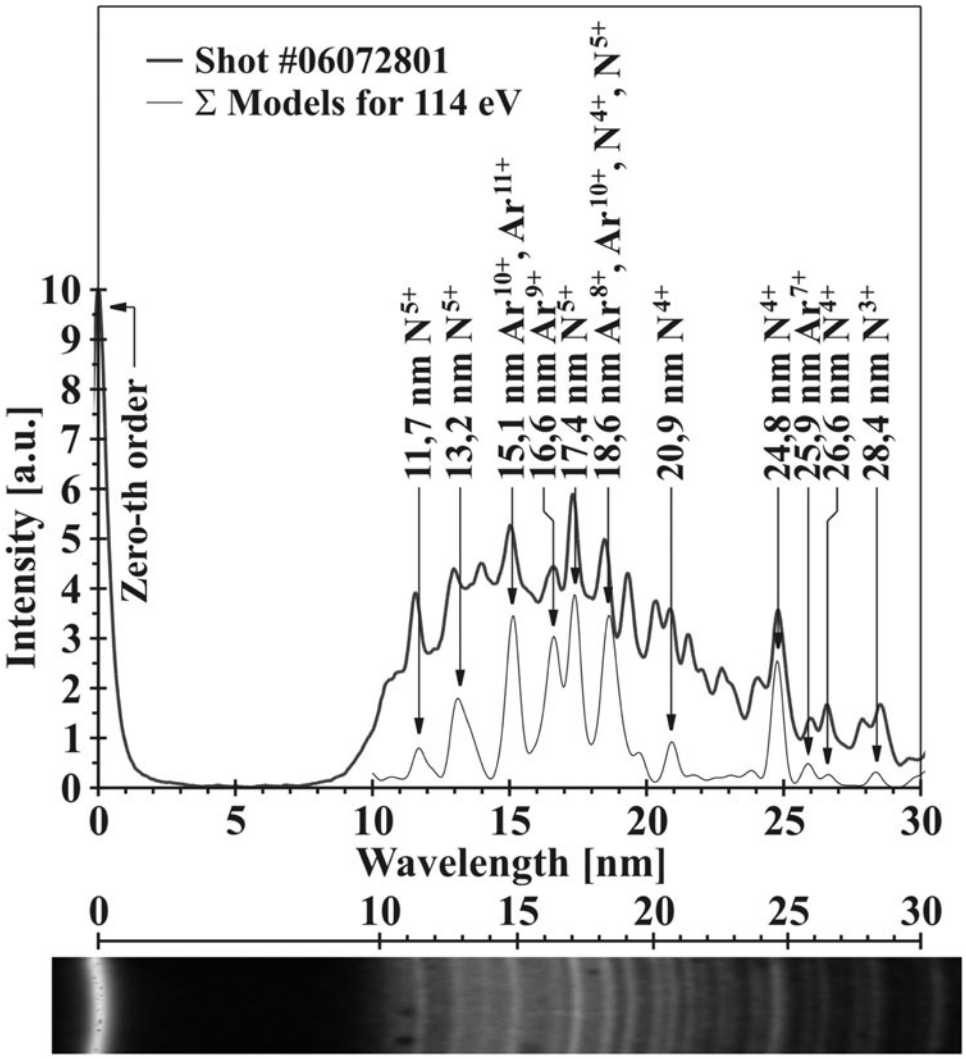

Fig. 5. Spectrum taken by flat field spectrograph, capillary filling nitrogen −200 Pa, gate 30 ns begins 46.6 ns after the current onset, current amplitude 56.3 kA.

input was first illuminated through a chopper (for preliminary adjustment), then by continuous light from a HeNe laser and the transmitted light was detected by the photomultiplier 65PK415. It turned out that initial fiber transmission at the shock wave compression phase falls and then (in the dilution phase) it rises (see Fig. 9, left). Unfortunately, sensitivity of this method to high pressures is very small (see Fig. 9, right). This method will be calibrated in a hydraulic press (in a quasi-static regime) as soon as it is available.

Wire Placed in Uncompressed Water and Exploded by a Slow Driver

Cu wire of different diameters (Ø0.1–0.3 mm) was exploded in a separately standing SHOW device. The explosion was performed by a slow driver (half period 4 μs) consisting of one or two condensers IK100-0.4/100 kV (400–800 nF charged to 60 kV), and a mechanical switch (see Fig. 10, left). The discharge current was "measured" by a Rogowski coil not optimized for this time-scale. Time-integrated pictures of wire explosion were taken in the visible range by a Canon EOS 350D Digital CCD camera. It turned out that plasma channel created in water by wire explosion remains (even in the case of this slow driver) all the time perfectly stable (see Fig. 10, right). This was a good promise for further experiments.

Wire Placed in Uncompressed Water and Exploded by a Fast Driver CAPEX-U

Recently the SHOW device was attached to the CAPEX-U facility (replacing the former capillary), and the first wire-explosions in non-compressed water were performed. The driving energy for wire explosion was nearly the same as in the former case of separately standing SHOW device and "slow" driving circuit (the water-filled coaxial pulse-forming line of the capacitance 12 nF was charged by

https://doi.org/10.1017/S0263034608000190 Published online by Cambridge University Press

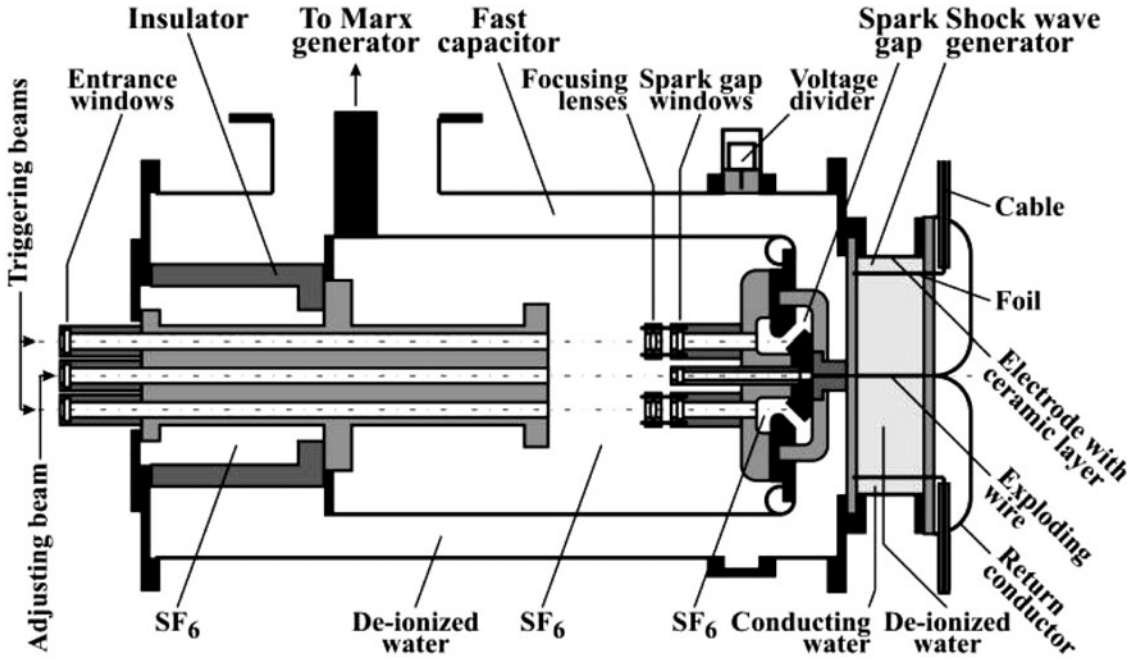

Fig. 6. CAPEX-U with the SHOW device.

Marx generator to the voltage ~450 kV, hence, the driving energy was ~1,22 kJ), but the characteristic time (current rise-time) was much shorter (~100 ns), and the current amplitude was as high as ~50 kA (see Fig. 11, left). The wire explosions were also photographed in the visible range. Contrary to explosions by the "slow" circuit, when the discharge channel appeared excellently stable, in the case of explosions by CAPEX-U (especially, if the high-voltage electrode was negative) some "hotter and colder regions" were visible. This sensitivity to polarity (different appearance if the high voltage electrode is positive or negative—see Fig. 11, right) may be attributed e.g., to transient hollow cathode effect, which in case of "slow" driving circuit may be hidden in quasi-stationary phase. In some cases (not shown here) the classical hot-spots were observed - caused probably by not straight enough primary wire (due to more difficult fixing in this case). Unfortunately, these last results are based on a few shots only, because preparation of the experiment was very laborious. Only recently we have developed some procedure that can speed up this process.

Finally, an axial radiation emission from exploded wire was investigated: the SHOW chamber was extended in axial direction by pneumatically controlled vacuum valve

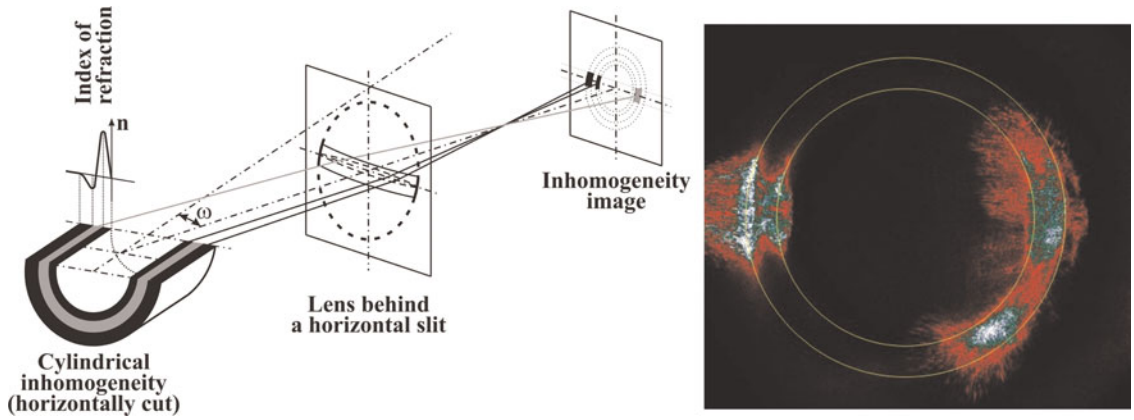

Fig. 7. (Color online) Schematic diagram of the off-axis shadowgraphy. Right: shadowgram of the shock wave; double-arc on the left depicts rising parts of the index of refraction (from undisturbed to the maximum, and from the minimum to undisturbed), single arc on the right shows falling part of index of refraction (from its maximum to its minimum); charging voltage 30 kV, probing time 111.4 μs, radius of the circle of maximum compression 16.2 mm, radius of the circle of maximum dilution 20.1 mm.

https://doi.org/10.1017/S0263034608000190 Published online by Cambridge University Press

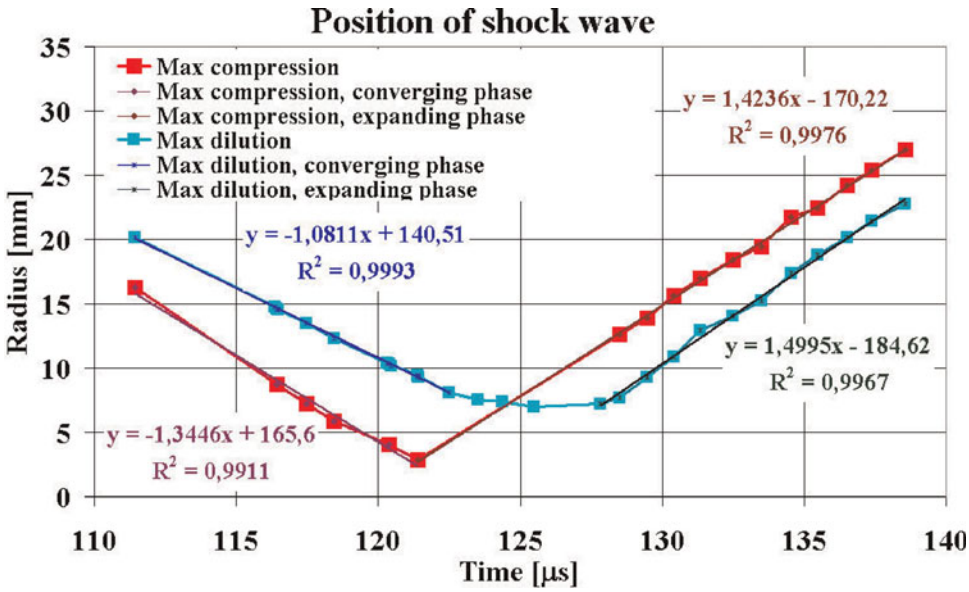

Fig. 8. (Color online) Position of the shock wave (charging voltage 30 kV).

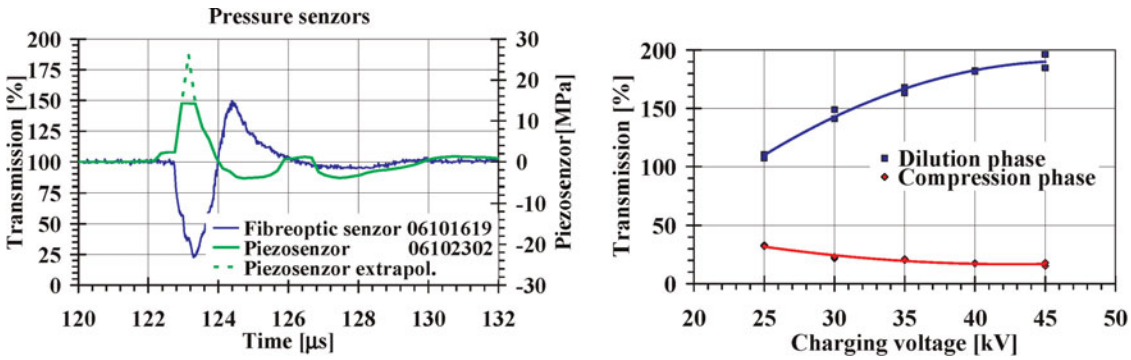

Fig. 9. (Color online) Left: Signal of fibre optic pressure sensor (blue curve) and piezo-sensor (green curve), charging 30 kV. Right: Transmission of fibre optic pressure sensor as a function of charging voltage; red curve corresponds to the first extreme (minimum), blue curve corresponds to the second extreme (maximum) of the signal of the fibre optic sensor.

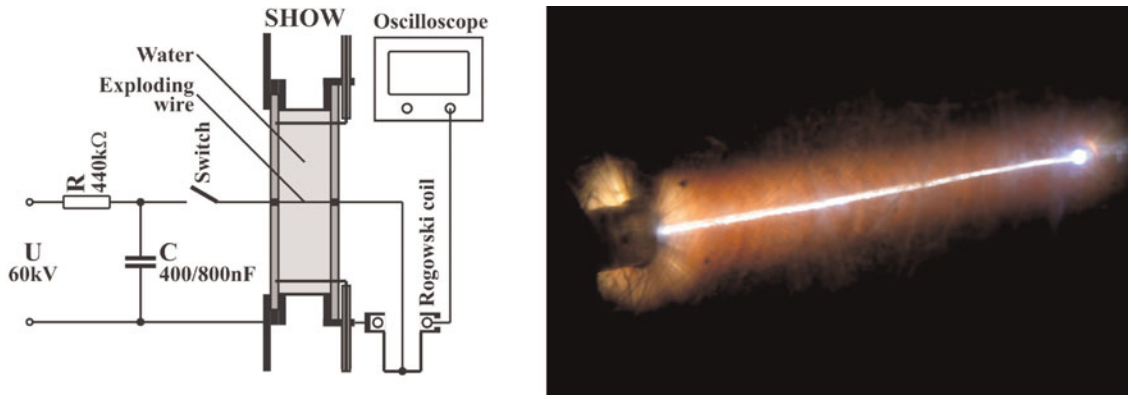

Fig. 10. (Color online) Left: Schematic diagram of the wire explosion with slow driver. Right: Time-integrated picture of wire explosion.

https://doi.org/10.1017/S0263034608000190 Published online by Cambridge University Press

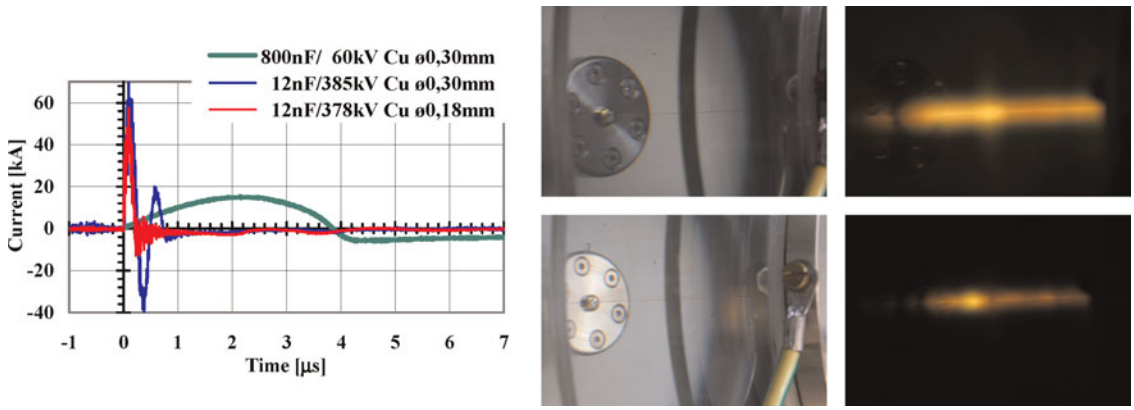

Fig. 11. (Color online) Left: Discharge current through the Cu exploding wire of the diameter 0.18 (red), and 0.3 mm (blue line); for comparison it is shown the discharge current through the exploding wire Ø0.3 mm driven by a "slow" circuit (dark green line). Right: Plasma of exploding wire: above – high voltage electrode is positive, below – high voltage electrode is negative; the bright "smeared" part in the central part of figures is due to circular not-polished trench in the PMMA flange (see left parts of the figures).

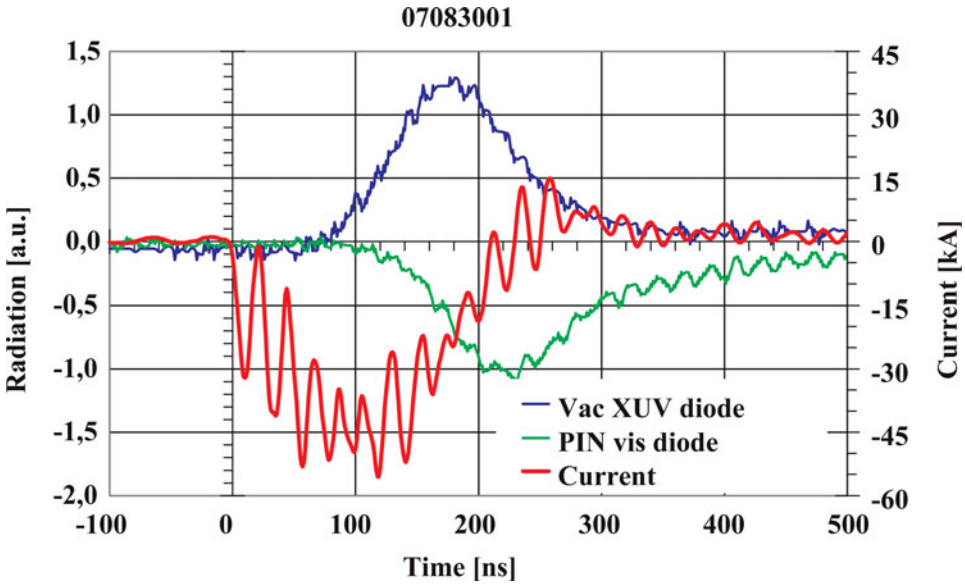

Fig. 12. (Color online) Signal of vacuum XUV photodiode with gold photocathode (blue solid line) and signal of PIN diode for visible range (green line); both detectors are placed at the end of axial evacuated drifting tube. Signal of Rogowski coil (red) indicates the current through the exploding wire. The Cu exploding wire has Ø0.18 mm.

and about 1 m long evacuated drifting tube. At the end of this tube both the vacuum photodiode with gold photocathode and the PIN diode for visible range were placed. Simultaneously, the current flowing through the exploding wire was detected by the Rogowski coil. Since a small viewing aperture is opened - only for narrow beam of paraxial rays, the initial corona glowing around the wire is not visible (see Fig. 12). Only as soon as the wire is evaporated and turned in a plasma channel (inclusive its relatively colder ends) the radiation can pass through the aperture and be registered by the detectors. However, in this moment (near the current maximum) it is already strongly heated and it radiates exclusively in the soft X-ray region. Only a few tens of nanoseconds later, when the plasma channel starts to cool-down also the visible radiation appears and lasts longer than the radiation in the soft X-ray region. This is to our knowledge for the first time when soft X-ray radiation from the discharge/exploding wire in water was measured. The future XUV spectroscopy measurements will provide information about approximate temperature and density of the plasma channel and about feasibility of this geometry for excitation or recombination pumping.

CONCLUSION

In the case of hydrogen-like nitrogen laser (which uses recombination pumping scheme) there are two opened questions: (1) how much discharge current will be required for excitation: ~80 kA as predicted by Vrba, or ~200 kA as predicted by the scaling laws (made on the bases of not fully justified prepositions: scaling leaves the rail of isoelectronic sequence) outlined in section 2; (2) will expansion cooling of previously pinched column be sufficiently fast to ensure building of population inversion? The first time-resolved

https://doi.org/10.1017/S0263034608000190 Published online by Cambridge University Press

spectroscopic measurements made at higher discharge current should give an answer to these questions.

In the case of nickel-like metal vapor laser (excitation pumping scheme) both previous questions ((1) question of sufficiently high power input, and (2) question of sufficiently fast compression that should guarantee detachment of the plasma column from the liquid wall) persist, but a third is added (3) if the wire (with solid-state density) results, after its expansion, in a suitable plasma density/plasma density profile. This work is in progress.

ACKNOWLEDGEMENT

The experimental part of this work was performed under auspices and with the support of the Grant Agency of the Czech Republic (contract 202/06/1324) and the Grant Agency of the Academy of Sciences CR (contracts KAN300100702 and KJB100430702), the theoretical part of this work was supported by the Ministry of Education, Youth, and Sports of the Czech Republic (contract 1P2004LA235 and LA08024).

REFERENCES

Ben-Kish, A., Shuker, M., Nemirovsky, R.A., Avni, U., Fisher, A., Ron, A. & Schwob, J.L. (2001). Investigating the dynamics of fast capillary discharges leads to soft X-ray laser realization at 46.9 nm. *J. Phys. IV* **11**, 99–102.

Boboc, T., Weigand, F. & Langhoff, H. (2000). Intensity enhancement of the C5+ Balmer radiation excited by capillary discharge pumping. *Appl. Phys. B* **70**, 399–405.

Bobrova, N.A., Bulanov, S.V., Esaulov, A.A. & Sasorov, P.V. (2000). Capillary discharge for guiding of laser pulses. *Plasma Phys. Rept.* **26**, 10–20.

Boss, T., Neff, W., Boboc, T., Weigand, F., Bischoff, R. & Langhof, H. (1998). Optical gain for the Ne VIII 4-3 transition by capillary discharge pumping. *J. Phys. D* **31**, 2472–2478.

Chilla, J.L.A. & Rocca, J.J. (1996). Beam optics of gain-guided soft–X-ray lasers in cylindrical plasma. *J. Opt. Soc. Am. B* **13**, 2841–2851.

Eberl, E., Wagner, T., Jacoby, J., Tauschwitz, A. & Hoffmann, D.H.H. (1997). Soft X-ray lasing at 519.7 angstrom in a recombining Z-pinch plasma. *Laser Part. Beams* **15**, 589–595.

Ehrlich, Y., Cohen, C., Zigler, A., Krall, J., Sprangle, P. & Esarey, E. (1996). Guiding of high intensity laser pulses in straight and curved plasma channel experiments. *Phys. Rev. Letters* **77**, 4186–4189.

Ellwi, S.S., Juschkin, L., Ferri, S., Kunze, H.-J., Koshelev, K.N. & Louis, E. (2001*a*). X-ray lasing as a result of an induced instability in an ablative capillary discharge. *J. Phys. D* **34**, 336–339.

Ellwi, S.S., Andreic, Z., Pleslic, S. & Kunze, H.-J. (2001*b*). Probing of the active layers in a capillary discharge soft X-ray laser at 18.22 nm. *Phys. Lett. A* **292**, 125–128.

Elton, R.C. (1990). *X-ray Lasers* Boston, MA: Academic Press, Inc.

Frati, M., Seminario, M. & Rocca, J.J. (2000). Demonstration of a 10-mJ tabletop laser at 52.9 nm in neonlike chlorine. *Opt. Lett.* **25**, 1022–1024.

Frati, M., Tomasel, F.G., Bowers, B., Gonzales, J.J., Shlyaptsev, V.N. & Rocca, J.J. (2001). Generation of highly ionised cadmium plasma columns for a discharge-pumped nickel-like Cd laser. *J. Phys. IV* **11**, 571–574.

Goltsov, A.Y., Korobkin, D.V., Ping, Y. & Suckewer, S. (2000). Transmission of laser radiation through microcapillary plasmas. *J. Opt. Soc. Am. B* **17**, 868–876.

Hayashi, Y., Xiao, Y., Sakamoto, N., Miyahara, H., Niimi, G., Watanabe, M., Okino, A., Horioka, K. & Hotta, E. (2003). Performance of Ne-like Ar soft X-ray laser using capillary Z-pinch discharge. *Jap. J. Appl. Phys.* **42**, 5285–5289.

Hildebrand, A., Kroger, M., Kunze, H.-J., Maurmann, S. & Ruhrmann, A. (1996). Amplified spontaneous emission on the $J = 2 \rightarrow 1$, 3p-3s transition of neon like argon in a capillary discharge. X-ray Lasers 1996, *Inst. Phys. Confer. Ser.* **151**, 187–191.

Hosokai, T., Kondo, S., Kando, M., Nakajima, M., Horioka, K. & Nakajima, K. (1999). Development of plasma wave-guide using fast capillary discharges. *Inst. Phys. Confer. Ser.* **159**, 179–182.

Jancarek, A., Pina, L., Vrbova, M., Tamas, M., Havlikova, R., Tomassetti, G., Ritucci, A. & Vrba, P. (2006). Nitrogen capillary discharge emission in 1.9–2.5 nm wavelength range. *Czechosl. J. Phys.* **56**, B250–B254.

Janulewicz, K.A., Rocca, J.J., Bortolotto, F., Sandner, W. & Nickles, P.V. (2000). Collisionally pumped hybrid soft X-ray laser in Ne-like sulphur. *Comptes Rendus A Sci IV Phys. Astrophys*, **1**, 1083–1092.

Janulewicz, K.A., Rocca, J.J., Bortolotto, F., Kalachnikov, M.P., Shlyaptsev, V.N., Wandner, W. & Nickles, P.V. (2001). Demonstration of a hybrid collisional soft-x-ray laser. *Phys. Rev. A* **6303**, 3803.

Janulewicz, K.A., Bortolotto, F., Lucianetti, A., Sandner, W., Nickles, P.V., Rocca, J., Bobrova, N. & Sasorov, P.V. (2003). Fast capillary discharge plasma as a preformed medium for longitudinally pumped collisional X-ray lasers. *J. Opt. Soc. Am B* **20**, 215–220.

Janulewicz, K.A., Schnurer, M., Tummler, J., Priebe, G., Risse, E., Nickles, P.V., Greenberg, B., Levin, M., Pukhov, A., Mandelbaum, A. & Zigler, A. (2005). Enhancement of 24.77-nm line emitted by the plasma of boron nitride capillary discharge irradiated by a high-intensity ultrashort laser pulse. *Opt. Lett.* **30**, 1572–1574.

Kaganovich, D., Ting, A., Moore, C.I., Zigler, A., Burris, H.R., Ehrlich, Y., Hubbard, R. & Sprangle, P. (1999). High efficiency guiding of terawatt subpicosecond laser pulses in a capillary discharge plasma channel. *Phys. Rev. E* **59**, R4769–R4772.

Kirsch, I., Choi, P., Larour, J. & Rous, J. (2001). Ultrafast hollow cathode triggered capillary discharge device as a strong XUV source. *J. Phys. IV* **11**, 605–608.

Kolacek, K. (2002). Principles and present state of capillary-discharge-pumped soft X-ray lasers. Proc. SPIE **5228** 27th ECLIM 2002, Moscow, Russia (Eds.: O.N. Krokhin, S.Yu. Guskov, Yu.A. Merkulev), 557–573.

Kolacek, K., Schmidt, J., Prukner, V., Sunka, P., Frolov, O., Straus, J. & Martinkova, M. (2005). Wire exploding in a focus of converging cylindrical shock wave in water – introductory remarks. IEEE 15th IPPC, Monterey, Ca., USA, June 13–17, Digest of Technical Papers 1976–2005, 280–283.

Korobkin, D.V., Nam, C.H., Suckewer, S. & Golstov, A. (1996). Demonstration of soft X-ray lasing to ground state in Li III. *Phys. Rev. Lett.* **77**, 5206–5209.

Koshelev, K.N. & Kunze, H.-J. (1997). Population inversion in a discharge plasma with neck-type instabilities. *Quan. Electron.* **27**, 164–167.

Kunze, H.-J., Koshelev, K.N., Steden, C., Uskov, D. & Wieschebrink, H.T. (1994). Lasing mechanism in a capillary discharge. *Phys. Lett. A* **193**, 183–187.

Kunze, H.-J., Ellwi, S.S. & Andreic, Z. (2005). Lasing in an ablative capillary discharge with structured return conductor. *Phys. Lett. A* **334**, 37–41.

Kunze, H.-J., Ellwi, S.S. & Andreic, Z. (2006). X-ray lasing in ablative capillary discharges. *Czechosl. J. Phys.* **56**, B280–B290.

Lee, K., Kim, J.H. & Kim, D. (2002). Analytical study of the dynamics of capillary discharge plasmas for recombination X-ray lasers using H-like ions. *Phys. Plasmas* **9**, 4749–4755.

London, R.A. (1988). Beam optics of exploding foil plasma X-ray lasers. *Phys. Fluids* **31**, 184–192.

Luther, B.M., Wang, Y., Berrill, M., Alessi, D., Marconi, M.C., Larotonda, M.A. & Rocca, J.J. (2005). Highly ionized Ar plasma wave guides generated by a fast capillary discharge. *IEEE Trans. Plasma Sci.* **33**, 582–583.

Milani, M., Ferraro, L., Causa, F. & Batan, D. (2007). Lasing properties and nonlinearities of dyes under high power pumping. *Laser Part. Beams* **25**, 557–566.

Nickles, P.V., Janulewicz, K.A., Rocca, J.J., Bortolotto, F., Lucianetti, A. & Wandner, W. (2001). Hybridly pumped collisional soft X-ray laser in Ne-like sulphur. *J. Phys. IV* **11**, 93–98.

Orlov, N.Y., Gus'kov, S.Y., Pikuz, S.A., Rozanov, V.B., Shelkovenko, T.A., Zmitrenko, N.V. & Hammer, D.A. (2007). Theoretical and experimental studies of the radiative properties of hot dense matter for optimizing soft X-ray sources. *Laser Part. Beams* **25**, 415–423.

Rahman, A., Hammarsten, E.C., Sakadzic, S., Rocca, J.J. & Wyart, J.F. (2003). Identification of $n = 4$, $\Delta n = 0$ transitions in the spectra of nickel-like cadmium ions from a capillary discharge plasma column. *Phys. Scripta* **67**, 414–419.

Ritucci, A., Tomassetti, G., Reale, A., Palladino, L., Reale, L., Flora, F., Mezi, L., Kukhlevsky, S.V., Faenov, A. & Pikuz, T. (2004). Investigation of a highly saturated soft X-ray amplification in a capillary discharge plasma wave guides. *Appl. Phys.* **78**, 965–969.

Rocca, J.J., Cortazar, O.D., Szapiro, B., Floyd, K. & Tomasel, F.G. (1993). Fast-discharge excitation of hot capillary plasmas for soft-x-ray amplifiers. *Phys. Rev. E* **47**, 1299–1304.

Rocca, J.J., Shlyaptsev, V., Tomasel, F.G., Cortazar, O.D., Hartshorn, D. & Chilla, J.L.A. (1994). Demonstration of a discharge pumped table-top soft X-ray laser. *Phys. Rev. Lett.* **73**, 2192–2195.

Rocca, J.J., Clark, D.P., Chilla, J.L.A. & Shlyaptsev, V.N. (1996*a*). Energy extraction and achievement of the saturation limit in a discharge-pumped table-top soft X-ray amplifier. *Phys. Rev. Lett.* **77**, 1476–1479.

Rocca, J.J., Clark, D.P., Tomasel, F.G., Shlyaptsev, V.N., Chilla, J.L.A., Benware, B., Moreno, C., Burd, D. & Gonzales, J.J. (1996*b*). Advances in discharge pumped soft X-ray lasers: From the observation of gain to achievement of the saturation limit and energy extraction. X-ray Lasers 1996, *Inst. Phys. Confer. Ser.* **151**, 176–183.

Rocca, J.J., Tomasel, F.G., Moreno, C.H., Shlyaptsev, V.N., Marconi, M.C., Benware, B.R., Gonzales, J.J., Chilla, J.L.A. & Macchietto, C.D. (1997). Progress in the development of table-top discharge-pumped soft X-ray lasers. *J. Phys. IV* **7**, 353–363.

Rocca, J.J. (1999). Table-top soft X-ray lasers. *Rev. Sci. Instrum.* **70**, 3799–3827.

Ruhl, F., Aschke, A. & Kunze, H.-J. (1997). Selective population of the $n = 3$ level of hydrogen-like carbon in two colliding laser-produced plasmas. *Phys. Lett. A* **225**, 107–112.

Sasaki, T., Yano, Y., Nakajima, M., Kawamura, T. & Horioka, K. (2006). Warm-dense-matter studies using pulse-powered wire discharges in water. *Laser Part. Beams* **24**, 371–380.

Schmidt, J., Kolacek, K., Frolov, O., Prukner, V. & Straus, J. (2006). Comparison of calculated and experimental results of CAPEX-U device. *Czechosl. J. Phys.* **56**, B371–B376.

Shin, H.J., Kim, D.O. & Lee, T.N. (1994). Soft-X-ray amplification in a capillary discharge. *Phys. Rev. E* **50**, 1376–1381.

Shuker, M., Ben-Kish, A., Fisher, A. & Ron, A. (2006). Titanium plasma source for capillary discharge extreme ultraviolet lasers. *Appl. Phys. Lett.* **88**, 026413.

Steden, C. & Kunze, H.-J. (1990). Observation of gain at 18.22 nm in the carbon plasma of a capillary discharge. *Phys. Lett. A* **151**, 534–537.

Straus, J., Kolacek, K., Bohacek, V., Frolov, O., Prukner, V., Ripa, M., Sember, V., Schmidt, J., Vrba, P. & Klir, D. (2004). Interactive system for the interpretation of atomic spectra. *Czechosl. J. Phys.* **54**, C314–C320.

Straus, J., Kolacek, K., Schmidt, J., Frolov, O. & Prukner, V. (2007). Computer generated spectra indicating parameters of capillary-discharge-plasma suitable to amplify radiation of Balmer-alpha transition of H-like N (13.4 nm). *Proc. 28th Int. Conf. on Phenomena in Ionized Gases*, Prague, CR, July 15–20, 1284–1285.

Tomasel, F.G., Shlyaptsev, V.N. & Rocca, J.J. (1996). Enhanced beam characteristics of a discharge-pumped soft-x-ray amplifier by an axial magnetic field. *Phys. Rev. A* **54**, 2474–2478.

Tomasel, F.G., Rocca, J.J., Shlyaptsev, V.N. & Macchietto, C.D. (1997). Lasing at 60.8 nm in Ne-like sulfur ions in ablated material excited by a capillary discharge. *Phys. Rev. A* **55**, 1437–1440.

Tomassetti, G., Ritucci, A., Reale, A., Palladino, L., Reale, R., Kukhlevsky, S.V., Flora, F., Mezi, L., Kaiser, J., Faenov, A. & Pikuz, T. (2002). Capillary discharge soft X-ray lasing in Ne-like Ar pumped by long current pulses. *Eur. Phys. J. D* **19**, 73–77.

Tomassetti, G., Ritucci, A., Reale, A., Palladino, L., Reale, L., Kukhlevsky, S.V., Flora, F., Mezi, L., Faenov, A., Pikuz, T. & Gaudieri, A. (2004). Toward a full optimization of a highly saturated soft-X-ray laser beam produced in extremely long capillary discharge amplifiers. *Opt. Commun.* **231**, 403–411.

Vrba, P., Vrbova, M., Bobrova, N.A. & Sasorov, P.V. (2005*a*). Simulation study of nitrogen soft X-ray capillary discharge laser. Proc. 9th IC X-ray Lasers, Beijing, China, May 24–28, 2004, X-ray Lasers 2004, *Inst. of Physics Conf. Series* **186**, 175–178.

Vrba, P., Vrbova, M., Bobrova, N.A. & Sasorov, P.V. (2005*b*). Modelling of a nitrogen X-ray laser pumped by capillary discharge. *Cent. Eur. J. Phys.* **3**, 564–580.

Vrba, P. & Vrbova, M. (2006). Population inversion during pinch decay in nitrogen capillary discharge. *Czechosl. J. Phys.* **56**, B425–B429.

Wong, C.S., Woo, H.J. & Yap, S.L. (2007). A low energy tunable pulsed X-ray source based on the pseudospark electron beam. *Laser Part. Beams* **25**, 497–502.

Wagner, T., Eberl, E. & Hoffmann, D.H.H. (1996*a*). Evidence for recombination XUV lasing at 52.0 nm and 49.8 nm in a fast, compact Z-pinch discharge. *Laser Part. Beams* **14**, 679–684.

Wagner, T., Eberl, E., Frank, K., Hartmann, W., Hoffmann, D.H.H. & Tkotz, R. (1996*b*). XUV amplification in a recombining z-pinch plasma. *Phys. Rev. Lett.* **76**, 3124–3127.

Wang, Y., Luther, B.M., Berrill, M., Marconi, M., Brizuela, F., Rocca, J.J. & Shlyaptsev, V.N. (2005). Capillary discharge-driven metal vapor plasma waveguides. *Phys. Rev. E* **72**, 061501.

Wyndham, E.S., Favre, M. & Aliaga-Rossel, R. (2006). The formation of metallic plasma in transient capillary discharges at high current. *Plasma Sour. Sci. & Techn.* **15**, 538–545.

Zou, X.B., Liu, R., Zeng, N.G., Han, M., Yuan, J.Q., Wang, X.X. & Zhang, G. X. (2006). A pulsed power generator for x-pinch experiments. *Laser Part. Beams* **24**, 503–509.

https://doi.org/10.1017/S0263034608000190 Published online by Cambridge University Press